HHS Public Access

Author manuscript

Cancer Prev Res (Phila). Author manuscript; available in PMC 2017 March 01.

Published in final edited form as:

Cancer Prev Res (Phila). 2016 March ; 9(3): 215–224. doi:10.1158/1940-6207.CAPR-15-0419.

Inhibition of Akt Enhances the Chemopreventive Effects of Topical Rapamycin in Mouse Skin

Sally E. Dickinson[1,2,*], **Jaroslav Janda**[1], **Jane Criswell**[1], **Karen Blohm-Mangone**[1], **Erik R. Olson**[1], **Zhonglin Liu**[3], **Christie Barber**[3], **Emanuel F. Petricoin III**[4], **Valerie S. Calvert**[4], **Janine Einspahr**[1,5], **Jesse E. Dickinson**[6], **Steven P. Stratton**[1,5], **Clara Curiel-Lewandrowski**[1,5], **Kathylynn Saboda**[1], **Chengcheng Hu**[1], **Ann M. Bode**[7], **Zigang Dong**[7], **David S. Alberts**[1,5], and **G. Timothy Bowden**[1,5,8]

[1]The University of Arizona Cancer Center, Tucson, Arizona

[2]Department of Pharmacology, The University of Arizona

[3]Department of Medical Imaging, The University of Arizona

[4]Center for Applied Proteomics and Molecular Medicine, George Mason University, Manassas, Virginia

[5]Department of Medicine, The University of Arizona

[6]Arizona Water Science Center, U.S. Geological Survey, Tucson, Arizona

[7]Department of Molecular Medicine and Biopharmaceutical Sciences, The Hormel Institute, The University of Minnesota, Austin, Minnesota

[8]Department of Cellular and Molecular Medicine, The University of Arizona

Abstract

The PI3Kinase/Akt/mTOR pathway has important roles in cancer development for multiple tumor types, including UV-induced non-melanoma skin cancer. Immunosuppressed populations are at increased risk of aggressive cutaneous squamous cell carcinoma (SCC). Individuals who are treated with rapamycin, (sirolimus, a classical mTOR inhibitor) have significantly decreased rates of developing new cutaneous SCCs compared to those that receive traditional immunosuppression. However, systemic rapamycin use can lead to significant adverse events. Here we explored the use of topical rapamycin as a chemopreventive agent in the context of solar simulated light (SSL)-induced skin carcinogenesis. In SKH-1 mice, topical rapamycin treatment decreased tumor yields when applied after completion of 15 weeks of SSL exposure compared to controls. However, applying rapamycin during SSL exposure for 15 weeks, and continuing for 10 weeks after UV treatment, increased tumor yields. We also examined whether a combinatorial approach might result in more significant tumor suppression by rapamycin. We validated that rapamycin causes increased Akt (S473) phosphorylation in the epidermis after SSL, and show for

[*]Corresponding author: Sally E. Dickinson, Ph.D., 1515 N. Campbell Ave., AZCC Room 3977, Tucson, AZ 85724, Phone: 520-626-6747, Fax: 520-626-4979, sdickinson@uacc.arizona.edu.

Conflict of Interest:
The authors declare that they have no conflict of interest.

the first time that this dysregulation can be inhibited *in vivo* by a selective PDK1/Akt inhibitor, PHT-427. Combining rapamycin with PHT-427 on tumor prone skin additively caused a significant reduction of tumor multiplicity compared to vehicle controls. Our findings indicate that patients taking rapamycin should avoid sun exposure, and that combining topical mTOR inhibitors and Akt inhibitors may be a viable chemoprevention option for individuals at high risk for cutaneous SCC.

Keywords

UV; skin; rapamycin; Akt; mTOR

Introduction

Nonmelanoma skin cancer (NMSC) is the most common malignancy worldwide and is rapidly increasing in incidence, representing an expanding public health burden of considerable magnitude [1–3]. NMSCs can be categorized as squamous cell carcinomas (SCCs) or basal cell carcinomas (BCCs), which account for approximately 16% and 80% of all skin cancers, respectively. The remaining 4% are accounted for primarily by melanomas. Cutaneous SCCs account for approximately 2,000 deaths per year in the United States, a number which is likely underreported [4, 5]. NMSCs are strongly associated with sun/ultraviolet (UV) light exposure. Natural sunlight contains 90–99% UVA (320–400 nm) and 1–10% UVB (200–280 nm), depending upon the geographic location. Despite increasing rates of sunscreen use, the effectiveness of this primary prevention approach may not be significant, possibly due to increased exposure times and inefficient re-application of sunscreens [6]. NMSCs also represent a major cause of morbidity after organ transplantation. SCCs are the most common cutaneous malignancies seen in this population, with a 65–100 fold greater incidence in organ transplant recipients compared to the general population [7]. Clearly, more effective prevention and treatment regimes for NMSC are required, especially for individuals at high risk.

Several signaling pathways have been implicated in the UV-mediated carcinogenesis process. Lately, the contribution of the serine/threonine protein kinase mTOR (mammalian target of rapamycin)has attracted attention in several types of cancer due to its ability to integrate stimuli from metabolites, extracellular signals and stressors to regulate translation, proliferation, and autophagy in the cell [8]. Phosphoinositide3-kinase (PI3K)/Akt/mTOR signaling is known to be dysregulated in several types of cancer, making the pathway a promising therapeutic target [9]. We and others have shown that UV light exposure induces PI3K/Akt/mTOR signaling along with mitogen activated protein kinases (MAPK) signaling in model systems and in human skin [10–15]. Dysregulation of PI3Kinase/Akt/mTOR signaling during the progression from normal skin to SCC has also been validated [16, 17]. The importance of careful regulation of this pathway in the skin is further supported in studies comparing the incidence of cutaneous SCCs in patients using cyclosporine A (CsA), versus the mTOR inhibitor rapamycin (sirolimus, a bacterial macrolide) as systemic immunosuppressants over time. In general, these studies found a significant protective effect

of rapamycin use against the development of new SCCs and other malignancies compared to those taking CsA during the study period [18–20].

However, the suitability of specifically targeting mTOR signaling in the fight against UV-induced skin cancer is currently uncertain. Early studies with rapamycin using adenocarcinoma-based xenografts in mice revealed dose-dependent inhibition of tumor growth, metastasis and angiogenesis compared to vehicle controls [21]. In contrast CsA, the most widely used immunosuppressive drug, increased tumor size and angiogenesis [21]. Although adverse events can make compliance difficult when rapamycin is administered systemically [20], a retrospective analysis suggests that oral dosing with this drug was an effective long-term therapy for patients suffering from tuberous sclerosis complex skin tumors [22]. Collectively, these studies suggest that rapamycin may be a promising preventive agent for populations at risk for certain skin malignancies.

When considering the options for drug delivery to the skin, topical application may be a reasonable approach for mTOR inhibitors in order to achieve local signaling pathway modulation while avoiding the challenges associated with systemic immunosuppression. Clinically, psoriasis and classic Kaposi's sarcoma have been successfully treated with topical rapamycin [23, 24]. In mouse models, topical pretreatment with rapamycin suppressed acute UVB-induced skin thickening by inhibiting epidermal proliferation [14]. However, the effects of topical mTOR inhibition in the context of solar UV-induced skin tumorigenesis has not been reported. Here we present the first study to examine rapamycin in the context of solar simulated light (SSL) treatment in mice. This study compares the effects of both concurrent rapamycin and SSL treatments (prevention) versus treating with UV to create tumor-prone skin, and then applying rapamycin (intervention). Crucially, the effect of co-treatment with rapamycin and the Akt inhibitor PHT-427 on tumor-prone skin is also presented.

Materials and Methods

Materials

Rapamycin was purchased from LC Laboratories (Woburn, MA). PHT-427 was donated by PHusis Therapeutics Inc. (San Diego, CA). Antibodies for Western blots were purchased from Santa Cruz Biotechnology (Dallas, TX; phospho-p70S6 Kinase T389 #sc-11759, total p70S6 #9379), Cell Signaling Technologies (Danvers, MA; phospho-Akt S473 #4060; phospho-mTOR S2448 #2971; α – tubulin #21285; phospho-S6 Ribosomal Protein #5364), or Sigma-Aldrich (St. Louis, MO; β – actin #A5441). All other reagents were obtained from Sigma-Aldrich.

Solar simulated light treatment

Female SKH-1 hairless mice at 5–8 weeks of age were purchased from Charles River Laboratories (Wilmington, MA) for chronic and acute solar simulated light (SSL) studies. All mouse studies were performed in accordance with protocols approved by the University of Arizona Institutional Animal Care and Use Committee (IACUC). SSL exposure was performed using a bank of 6 UVA340 bulbs (Q-lab Corporation, Cleveland, OH). Fluence

intensity was determined using an ILT 1700 Radiometer equipped with UVA and UVB meters (International Light Technologies, Peabody, MA). Output of the bulbs was determined to be 93% UVA and 7% UVB.

Acute solar UV exposures used a dose of 105 kJ/m^2 UVA/6.4 kJ/m^2 UVB. Mice (n = 3) were then sacrificed at the appropriate timepoints and their back skins were harvested and snap frozen. The frozen epidermis was then scraped, lysed and sonicated as described for Western blot analysis [25]. For some acute experiments, mice were treated topically on their backs from the shoulder blades to the top of the hips with agents (rapamycin or PHT-427) dissolved in 200uL of acetone 48hr prior, 24hr prior, and 1hr prior to the SSL exposure.

For tumorigenesis studies (n = 20), mice were exposed to SSL three times a week. Upon receipt from Charles River Laboratories, mice were randomly assigned to treatment groups. The number of mice per group (20) was calculated to provide enough power to detect a 50% decrease in tumor multiplicity with 95% confidence. UV exposures were initiated at 15.4 kJ/m^2 UVA/1.2 kJ/m^2 UVB and increased by 10% weekly until a holding dose of38.5 kJ/m^2 UVA/2.8 kJ/m^2 UVB was reached at week 10. After week 15, UV treatments were stopped at a cumulative dose of 427 kJ/m^2 UVA/33 kJ/m^2 UVB. Mice were weighed and observed weekly, and tumors were recorded at first detection, typically after week 15. Tumor burden (area) was calculated by multiplying the length by the width of each tumor in millimeters. Average tumor burden was calculated by dividing the sum of the individual tumor burdens each week by the number of the mice in the treatment group. Multiplicity was defined as the sum of the tumors for each treatment group divided by the number of mice in that group each week. Mice were always sacrificed 24hr after their final drug treatment. No adverse reactions or changes in group weekly weights due to drug applications were observed.

Rapamycin prevention/intervention tumorigenesis study—The acetone control group received topical applications of 200uL acetone (vehicle) on the treatment area 1hr prior to each SSL treatment (15 weeks), which then continued three times a week until the end of the study. The treatment area on each mouse was defined as the back skin from the shoulder blades to the top of the hips. The rapamycin prevention group, which could also be referred to as the “early and protracted treatment” group, received topical rapamycin (50nmol/back) in 200uL acetone 1hr prior to each SSL exposure and continuing three times a week after UV stopped. The rapamycin intervention group received topical acetone treatments 1hr prior to each SSL exposure and then switched to topical rapamycin treatments three times a week after UV stopped (i.e., a “post UV” group).

Rapamycin+PHT-427 intervention tumorigenesis study—In this experiment all mice received no treatment during the 15 weeks of solar UV exposure, then were split into four groups: acetone (vehicle) control, rapamycin (50nmol/back), PHT-427 (3.7 umol/back), or rapamycin + PHT-427 (same doses). All drugs were applied topically in 200uL three times a week until sacrifice.

Reverse Phase Protein Microarray (RPPA) analysis

Epidermal proteins from naïve female SKH- 1 mice treated acutely with SSL were processed for RPPA analysis according to established protocols [16]. Briefly, frozen back

skin was scraped and ground to powder using a frozen mortar and pestle. The powder was then lysed using a 1:1 mixture of T-PER Tissue Protein Extraction Reagent (Pierce) and 2× Tris-Glycine SDS Sample Buffer (Invitrogen) containing 5% β-mercaptoethanol. RPPAs were prepared with an Aushon 2470 solid pin microarrayer (Aushon Biosystems). Slides were stained with a set of 40 antibodies against phospho-specific and total proteins. All antibodies were subjected to extensive validation for single band, appropriate MW specificity by Western blot as well as phosphorylation specificity through the use of cell lysate controls. Antibody and Sypro Ruby stained slides were scanned on a Tecan laser scanner (TECAN, Mönnedorf, Switzerland) using the 620 nm and 580 nm weight length channel respectively. Images were analyzed with MicroVigene Software Version 5.1.0.0 (Vigenetech, Carlisle, MA) as previously described [26]. In brief, the software performs spot finding along with subtraction of the local background and unspecific binding generated by the secondary antibody. In addition, the program automatically normalizes each sample to the corresponding amount of protein derived from Sypro Ruby stained slides and averages the triplicates.

SPECT imaging for apoptosis *in vivo*

Female SKH-1 hairless mice were treated topically with vehicle (acetone, n = 7) or rapamycin (50 nmol/back, n = 9) at 48hr, 24hr and 1hr prior to an acute SSL exposure as described above and imaged 48hr later. An additional group of SKH-1 mice received no treatment as controls (n = 6). The mice of the three groups were imaged with ^{99m}Tc-duramycin, which is a molecular probe binding to externalized membrane phosphatidylethanolamine (PE) on apoptotic cells. Upon binding to PE, ^{99m}Tc-duramycin becomes deposited in cellular membranes [27–30]. Using instant labeling kits obtained from Molecular Targeting Technologies, Inc. (West Chester, PA), ^{99m}Tc-duramycin was produced on site by incubating 500 μl of ^{99m}Tc-pertechnetate saline (~555 MBq) with 15 μg 6-hydrazinopyridine-3-carboxylic acid (HYNIC) conjugated duramycin (HYNIC-duramycin), 30 mg tricine and 10 mg trisodium triphenylphosphine-3,3’,3”-trisulfonate as co-ligands, as well as 15 μgtin chloride dihydrate, at 80°C for 30 minutes. Two hours after intravenous injection of 17.5–37.0 MBq ^{99m}Tc-duramycin (0.2 mL, radiochemical purity > 99%), anesthetized mice were imaged with a high-resolution SPECT imager called FastSPECT II using a multi-bed acquisition protocol to generate whole body tomographic images.

At the end of each imaging session, the mice were sacrificed, and back and belly skin about 6–9 cm^2 in size were harvested and weighed. The radioactivity was measured by a dose calibrator to calculate the percentage of injected dose per gram of tissue (%ID/g). Subsequently the tissue samples were laid on phosphate plates at 4 C° for 5 minutes of autoradiograph exposure. The digital autoradiographs of skin tissues were read with a Fujifilm BAS-5000 reader.

Keratinocyte cell culture

Adult human primary epidermal keratinocytes were cultured in EpiLife media (MEPI500CA) supplemented with HKGS (S0015), purchased from ThermoFisher Scientific (Waltham, MA), grown at 37°C in 5% CO_2, and used within three passages. Cells were

starved of growth factor for 24 hr prior to treatment with agents. HaCaT human immortalized keratinocytes [31–33] were cultured in DMEM containing 10% fetal bovine serum (FBS) and 100 units/mL penicillin/streptomycin at 37°C in 5% CO_2. HaCaT cells were routinely tested for mycoplasma but were not authenticated. For treatments, media was changed to serum-free DMEM including antibiotics and DMSO or drug for the indicated times.

Western blot analysis

Frozen back skin was scraped with a razor blade in order to remove the epidermis, which was ground to a powder as described for RPPA. The powder was then lysed and sonicated for Western blot analysis [16]. Cultured keratinocytes were lysed in RIPA lysis buffer including 1× HALT phosphatase/protease inhibitors (Invitrogen, Waltham, MA) and briefly sonicated on ice as described [34]. Protein concentration was determined using the Dc protein assay for both skin and cell culture lysates (BioRad, Hercules, PA). Lysates were separated by SDS PAGE, transferred to PVDF membranes, blocked and probed with primary and secondary antibodies as described [34]. For keratinocytes, western blots shown are representative of n = 3. For back skins, data are representative of n = 2 (3–4 mice/group). All phospho-protein related images are from fresh blots. Loading controls were performed on relevant stripped blots.

Statistical Analysis

Means, standard deviations and other summary statistics were calculated by treatment group for all outcome measurements. Primary analysis compared end of study total tumor burden and total tumor counts (multiplicity) among the 4 treatment groups in the two rapamycin tumorigenesis studies. In the rapamycin prevention/intervention tumorigenesis study the primary analysis compared end of study total tumor burden and total tumor counts (multiplicity) among the 2 treatment groups and an acetone control group. Cross-sectional analyses used the Mann-Whitney or Wilcoxon Rank-sum Test. Uncorrected p-values are presented for these cross-sectional analyses.

After appropriate transformations to achieve approximate normality, mixed effect models were fit for tumor burdens to test for differences over time by treatment groups and to measure subject specific variability. A random slope was added to account for different growth rates between mice.

Tumor counts data were analyzed using a mixed effects poisson model to test for differences over time by treatment groups and to measure subject specific variability. A random slope was added to account for different growth rates between mice. Stata V14 was used for all statistical analysis.

Results

Acute SSL treatment activates mTOR/Akt signaling pathways in mouse epidermis

Treatment of SKH-1 hairless mice with an acute dose of SSL resulted in rapid phosphorylation of Akt (S473) and mTOR (S2448), with subsequent phosphorylation of

downstream p70S6Kinase. These responses were evident as soon as the acute treatment stopped (0hr, or about 90 min under the bulbs), peaking for mTOR at 1hr post UV and declining by 4hr post UV (Figure 1A, 8hr and 24hr not shown). The same epidermal samples were subjected to RPPA protein pathway activation analysis and individually tested for the activation and/or expression of multiple phospho and total proteins within the Akt-mTOR signaling pathway as kinases and their known substrates (Figure 1B). Triplicate averages for representative proteins are shown on the heat map, where red indicates an increase in signal (phosphorylation or total protein) and green indicates a decrease in signal (a selection of mTOR related proteins is shown here). With unsupervised clustering, the heat map indicates that the highest phosphorylation/protein levels were at the 0hr and 30min time points, and the least signal was found in the no UV control samples. The schema depicted in Figure 1B represents the linkages between the mTOR/Akt-related proteins shown in the heat map.

Blocking SSL-induced mTOR signaling with topical rapamycin causes schedule-dependent outcomes in mouse skin tumorigenesis

We chose to inhibit mTOR function using the immunosuppressant rapamycin in a chemoprevention experiment with three arms: acetone control, rapamycin prevention and rapamycin intervention. The control group received topical acetone prior to each SSL exposure and then continued the acetone treatments three times a week until sacrifice at week 25, yielding a final tumor multiplicity of 5.5 tumors/mouse and burden of 9.2 mm^2 (Figure 2A). Treatment with acetone during UV exposure followed by rapamycin after UV stopped at week 15 (rapamycin intervention on tumor prone skin) resulted in a lower average tumor multiplicity (3.7 tumors/mouse) and average tumor burden (4.9 mm^2) when compared to the acetone control animals. In contrast, treatment with rapamycin both during the 15 weeks of solar UV exposure and for an additional 10 weeks post UV (rapamycin "prevention") resulted in higher tumor multiplicity (7.2 tumors/mouse) as well as greater tumor burden (12.6 mm^2) compared to the acetone control. While there is a statistically significant difference in absolute tumor multiplicity and burden between the two rapamycin treatment arms ($p = 0.009$ for multiplicity, $p < 0.001$ for burden), these arms are not individually significantly different from the acetone control. However, mixed model analysis indicates that the slopes of the multiplicity and burden curves for the treatment groups are each significantly different than the acetone control group ($p < 0.001$).

Rapamycin enhances SSL-induced apoptosis in the skin as imaged *in vivo*

Focal accumulation (hot spots) of ^{99m}Tc-duramycin in the back skin was notably visualized in all mice that received SSL exposure after 48 hours. In contrast, no focal radioactive spots were detectable in the skin of control (no UV) mice. In the mice treated with rapamycin before SSL exposure, all SPECT images showed more hot spots spreading over the back skin with higher radioactivity compared to the hot spots visualized in the mice treated with vehicle. Representative displays from reconstructed FastSPECT II skin images of ^{99m}Tc-duramycin are shown in Figure 3A (top row). The hot spot uptake of ^{99m}Tc-duramycin on the mouse skin with SSL exposure was confirmed by digital autoradiograph imaging as shown in the bottom row of Figure 3A.

The results of biodistribution measurements (%ID/g) of harvested back skin and belly skin are presented in Figure 3B, in which the skin radioactivity of those of mice treated with SSL and SSL plus rapamycin were significantly high relative to that of control mice. Moreover, radioactive uptake of ^{99m}Tc-duramycin in the group with SSL plus rapamycin was higher than that in the SSL plus acetone group. The overall uptake of ^{99m}Tc-duramycin in the back skin of mice with SSL and SSL plus rapamycin was significantly higher than that in the belly skin.

Akt (S473)stimulation by rapamycin can be inhibited by PHT-427 treatment in cell culture

Recent literature suggests that a side-effect of rapamycin treatment is dysregulation of Akt signaling [35]. We therefore examined the effect of rapamycin on Akt phosphorylation in keratinocytes, and tested whether an Akt inhibitor, PHT-427 could block these effects. PHT-427 is a pleckstrin homology domain inhibitor which has been shown to block both Akt and PDK1 activity in multiple cell types [36, 37]. Rapamycin induced a time and dose-dependent increase in Akt (S473) expression in cultured primary human keratinocytes (Figure 4A, 4B). This is matched by correlative inhibition of S6 Ribosomal Protein phosphorylation, indicating blockade of mTOR activity. However, co-treatment with PHT-427 significantly reduced rapamycin-induced Akt (S473) phosphorylation after 24hr in HaCaT keratinocytes(Figure 4C).

Topical rapamycin treatment causes delayed hyperphosphorylation of Akt (S473) which is blocked by PHT-427 co-treatment in the epidermis

Female SKH-1 mice were pretreated with vehicle or rapamycin (50nmol/back) three times over the course of two days. The mice were then acutely exposed to SSL as in Figure 1 and harvested over a timecourse of 0hr to 4hr post UV for analysis of Akt signaling. Western blot analysis shows that rapamycin pretreatment caused significant inhibition of SSL-induced phosphorylation of S6 Ribosomal Protein, a marker of mTOR activity, at all timepoints (Figure 5A). Early timepoints after SSL treatment indicate that rapamycin caused reduced Akt (S473) phosphorylation compared to vehicle controls, but at 4 hr post SSL this trend is reversed, and the rapamycin treated skins show slightly greater Akt (S473) phosphorylation than vehicle controls (Figure 5A). In a second, independent experiment, mice were treated exactly as in figure 5A, but harvested at 6 hr and 24hr post UV in order to verify the previous findings and test their duration. As is shown in Figure 5B, at 6hr post SSL rapamycin pretreatment caused a significant increase in Akt (S473) phosphorylation compared to vehicle+SSL controls. UV-induced phosphorylation of S6 Ribosomal Protein is still strongly inhibited by rapamycin at this time, indicating that the agent is still functional in the skin. At 24hrpost SSL, rapamycin is still able to inhibit UV-induced phosphorylation of S6 Ribosomal Protein, and Akt (S473) phosphorylation levels are still slightly higher than the vehicle+SSL control. Notably, at 24hr the skins treated with rapamycin but no UV have greater Akt (S473) expression than the vehicle no UV controls (Figure 5C). A third acute *in vivo* experiment was performed to examine whether PHT-427 could inhibit SSL-induced Akt (S473) phosphorylation and possibly the stimulatory effects of rapamycin on this protein in the skin. Mice were treated three times with rapamycin (50nmol/back) or PHT-427 (3.7umol/back), both agents, or vehicle prior to an acute dose of SSL as in Figure 1 and were harvested 6hr later. Epidermal lysates from this trial recapitulate the above

findings that rapamycin enhances SSL-induced Akt (S473) phosphorylation. Treatment with PHT-427 moderately inhibited SSL-induced Akt (S473) phosphorylation, but combining PHT-427 with rapamycin dramatically reduced the stimulatory effect of rapamycin on Akt (S473), reducing its expression to nearly vehicle control+SSL levels (Figure 5D).

Co-treatment of rapamycin with PHT-427 additively inhibits SSL-induced skin tumorigenesis in mice

To determine the effects of rapamycin treatment alone or in combination with the PHT-427 on SSL-induced skin tumorigenesis, animals were exposed to 15 weeks of solar UV followed by 10 weeks of topical treatment with either acetone, rapamycin (50nmol/back), PHT-427 (3.7umol/back), or rapamycin and PHT-427. Both rapamycin and PHT-427 mildly reduced tumor multiplicity as compared to the acetone control (2.3 or 2.1 tumors/mouse for rapamycin or PHT-427 respectively, versus 2.9 tumors/mouse for acetone, Figure 6), but this inhibition did not reach statistical significance. Importantly, when the two agents are combined, tumor multiplicity was reduced by more than 50%, a significant outcome (1.4 tumors/mouse, $p = 0.03$). Tumor burden followed the same trend, with the combination of the two agents inhibiting tumor volume more dramatically than each agent alone, resulting in a significant reduction in the slopes of the curves ($p = 0.01$), if not a significant inhibition of the absolute tumor burden numbers between the acetone control group and the rapamycin +PHT group ($p = 0.089$). This outcome is likely due to high variability of final tumor burden in the acetone control group for this experiment.

Discussion

In the current study, we examine the effects of topical application of rapamycin in the context of SSL-induced skin tumorigenesis using both naïve and “tumor prone” mouse models. The results of this direct comparison strikingly delineate a schedule-dependent outcome on tumor burden and multiplicity in SSL-exposed SKH-1 mice in which co-treatment is detrimental while post-treatment is protective. These dualistic findings corroborate those of previous trials in which SKH-1 mice were exposed to UVB and treated with rapamycin by i.p. injection [38, 39]. However, the co-treatment protocol was in fact protective when rapamycin was used in dietary form during UV exposure or topically during two-stage chemical carcinogenesis [40, 41]. This raises the possibility that dietary effects and tumor stimulus may contribute to the outcome of rapamycin treatment in the skin. However, our results confirm that topical application of nanomolar amounts of rapamycin have significant effects on epidermal response to UV/tumorigenesis on the same order as that found in i.p. models (2mg/kg) in the same strain of mice. Topical application of rapamycin may therefore be a treatment option for some immunosuppressed patients at high risk for cutaneous SCC yet unable or unwilling to switch their current systemic regimen.

Imaging results *in vivo* show that rapamycin treatment caused a substantial potentiation of acute SSL-induced apoptotic signaling. SSL treatment induced a punctate pattern of radiolabeled duramycin to appear on back skin which significantly increased with rapamycin exposure. This trend, and the significance thereof, was confirmed using autoradiography of harvested back and belly skin. The increase in apoptosis due to rapamycin treatment of the

skin is in contrast to findings of Carr et al., who did not find any effects on UVB-induced apoptosis due to rapamycin exposure [14]. However, there is substantial precedence in the literature for a pro-apoptotic effect of rapamycin in other tissue types [42, 43]. Our findings may differ from Carr et al. due to *in vivo* or dosage effects, and we are pursuing this interesting finding further.

The role of Akt in rapamycin-treated systems has recently become a subject of interest for cancer research. Our results indicate that inhibition of mTOR using rapamycin caused dysregulation of Akt signaling in keratinocyte cell culture and in mouse skin. There is a reproducible, delayed rapamycin-dependent hyperphosphorylation of Akt (S473) in mouse epidermis in response to acute treatment with SSL. This finding is supported by recent studies indicating that treatment with rapamycin causes subsequent release of a negative feedback loop to IRS1, resulting in increased PI3Kinase/Akt signaling in several cell types [35, 44, 45] (Supplementary Figure 1). Similar rapamycin-dependent epidermal dysregulation of Akt (S473) phosphorylation in the presence of UV or TPA is also noted in the literature [14, 41]. Our data, however, are the first to clearly delineate the etiology of this dysregulation*in vivo* and to demonstrate inhibition of this effect using an Akt inhibitor (PHT-427) in the skin.

The combination of rapamycin and PHT-427 was also found to have a significant additive effect on inhibition of tumor multiplicity in SSL- treated tumor-prone skin. It should be noted that the trends in the data near the end of the measurements suggest that, given time, these tumors could have developed resistance to one or both of the agents being tested. Increasing tumor volume could also affect the ability of the topical agent(s) to penetrate into the larger tumors. Future studies may benefit from a higher dose of both rapamycin and PHT-427, since neither agent caused any observed toxicities or disturbances in weight (data not shown). Notably, the current data provides evidence that blocking both mTOR and PDK/Akt signaling in UV-induced tumor-prone skin causes significant delays and decreases in tumorigenesis. Topical combinatorial therapy with agents such as these should therefore be considered for possible clinical use in immunosuppressed individuals at high risk for cutaneous SCCs.

The observation that treatment with rapamycin concurrently with solar UV caused increased tumor multiplicity and burden in our topical model (the “prevention” arm of Figure 2) and in the literature with i.p. injections suggests not only that patients taking rapamycin may need to dramatically reduce their sun exposure. It evokes several more questions that require careful clinical testing. For instance, the possibility that UV may catalyze the conversion of topical rapamycin to tumorigenic metabolites should be addressed. In addition, the fact that immunosuppressed patients who switched from CsA to rapamycin dramatically reduced their risk of developing future SCCs (as long as they did not have multiple SCCs before conversion) is in alignment with the “intervention” model findings in Figure 2, which is supported by other treatment regimes [39, 41]. Additional studies in SKH-1 mice have found that dietary CsA exposure during UV protected against skin tumorigenesis, while post-UV dietary CsA had no effect and bolus treatments with the agent during UV increased tumor burden [46]. It is therefore possible that continuous versus intermittent dosing with rapamycin may also have differing effects on tumor outcomes. In addition, recent studies

with mice have discovered that circadian rhythm can affect immune responses [47, 48]. Overall, the schedule dependent effect found in Figure 2 and the additive inhibition of tumorigenesis seen with rapamycin+PHT-427 treatment support confidence that future clinical evaluations will identify optimal treatment schedules/combinations on an individual basis to support immunosuppression and reduce the risk of developing skin lesions in high-risk populations.

Supplementary Material

Refer to Web version on PubMed Central for supplementary material.

Acknowledgments

Grant Support:

This work was supported by the following NIH grants: NCI P01 CA023074 (S.E. Dickinson, J. Janda, J. Criswell, K. Blohm-Mangone, E.R. Olson, J.J. Rusche, J. Einspahr, S.P. Stratton, C. Curiel-Lewandrowski, K. Saboda, C. Hu, A.M. Bode, Z. Dong, D. Alberts, G.T. Bowden), P30 CA027502 (all University of Arizona Cancer Center members)and NIBIB P41-EB002035 (C. Barber, Z. Liu).

We thank PHusis Therapeutics Inc. for their gift of the PHT-427 compound and Drs. Terry Landowski and Georg Wondrak for critical review of the manuscript. We thank Marlon Taylor and Nichole Burkett for sample processing. We thank Jadrian Rusche for tireless efforts with technical support and tumor measurements, may he rest in peace. The use of brand names does not constitute endorsement by the U.S. Geological Survey.

References

1. Liu LS, Colegio OR. Molecularly targeted therapies for nonmelanoma skin cancers. Int J Dermatol. 2013; 52:654–665. [PubMed: 23679874]
2. Wondrak GT. Sunscreen-based skin protection against solar insult: molecular mechanisms and opportunities. Fundamentals of Cancer Prevention. 2014; 30:301–320.
3. Natarajan VT, Ganju P, Ramkumar A, Grover R, Gokhale RS. Multifaceted pathways protect human skin from UV radiation. Nat Chem Biol. 2014; 10:542–551. [PubMed: 24937072]
4. Housman TS, Feldman SR, Williford PM, Fleischer AB Jr, Goldman ND, Acostamadiedo JM, et al. Skin cancer is among the most costly of all cancers to treat for the Medicare population. J Am Acad Dermatol. 2003; 48:425–429. [PubMed: 12637924]
5. American Cancer Society. Cancer Facts & Figures 2013. American Cancer Society; 2013.
6. Autier P, Boniol M, Dore JF. Sunscreen use and increased duration of intentional sun exposure: still a burning issue. Int J Cancer. 2007; 121:1–5. [PubMed: 17415716]
7. Chockalingam R, Downing C, Tyring SK. Cutaneous squamous cell carcinomas in organ transplant recipients. J Clin Med. 2015; 4:1229–1239. [PubMed: 26239556]
8. Strozyk E, Kulms D. The role of AKT/mTOR pathway in stress response to UV-irradiation: implication in skin carcinogenesis by regulation of apoptosis, autophagy and senescence. Int J Mol Sci. 2013; 14:15260–15285. [PubMed: 23887651]
9. Polivka J Jr, Janku F. Molecular targets for cancer therapy in the PI3K/AKT/mTOR pathway. Pharmacol Ther. 2014; 142:164–175. [PubMed: 24333502]
10. Bachelor MA, Cooper SJ, Sikorski ET, Bowden GT. Inhibition of p38 mitogen-activated protein kinase and phosphatidylinositol 3-kinase decreases UVB-induced activator protein-1 and cyclooxygenase-2 in a SKH-1 hairless mouse model. Mol Cancer Res. 2005; 3:90–99. [PubMed: 15755875]
11. Bowden GT. Prevention of non-melanoma skin cancer by targeting ultraviolet-B-light signalling. Nat Rev Cancer. 2004; 4:23–35. [PubMed: 14681688]

12. Liu K, Yu D, Cho YY, Bode AM, Ma W, Yao K, et al. Sunlight UV-induced skin cancer relies upon activation of the p38alpha signaling pathway. Cancer Res. 2013; 73:2181–2188. [PubMed: 23382047]
13. Syed DN, Afaq F, Mukhtar H. Differential activation of signaling pathways by UVA and UVB radiation in normal human epidermal keratinocytes. Photochem Photobiol. 2012; 88:1184–1190. [PubMed: 22335604]
14. Carr TD, DiGiovanni J, Lynch CJ, Shantz LM. Inhibition of mTOR suppresses UVB-induced keratinocyte proliferation and survival. Cancer Prev Res (Phila). 2012; 5:1394–1404. [PubMed: 23129577]
15. Bermudez Y, Stratton SP, Curiel-Lewandrowski C, Warneke J, Hu C, Bowden GT, et al. Activation of the PI3K/Akt/mTOR and MAPK signaling pathways in response to acute solar-simulated light exposure of human skin. Cancer Prev Res (Phila). 2015; 8:720–728. [PubMed: 26031292]
16. Einspahr JG, Calvert V, Alberts DS, Curiel-Lewandrowski C, Warneke J, Krouse R, et al. Functional protein pathway activation mapping of the progression of normal skin to squamous cell carcinoma. Cancer Prev Res (Phila). 2012; 5:403–413. [PubMed: 22389437]
17. Chen SJ, Nakahara T, Takahara M, Kido M, Dugu L, Uchi H, et al. Activation of the mammalian target of rapamycin signalling pathway in epidermal tumours and its correlation with cyclin-dependent kinase 2. Br J Dermatol. 2009; 160:442–445. [PubMed: 19016696]
18. Kauffman HM, Cherikh WS, Cheng Y, Hanto DW, Kahan BD. Maintenance immunosuppression with target-of-rapamycin inhibitors is associated with a reduced incidence of de novo malignancies. Transplantation. 2005; 80:883–889. [PubMed: 16249734]
19. Alberu J, Pascoe MD, Campistol JM, Schena FP, Rial Mdel C, Polinsky M, et al. Lower malignancy rates in renal allograft recipients converted to sirolimus-based, calcineurin inhibitor-free immunotherapy: 24-month results from the CONVERT trial. Transplantation. 2011; 92:303–310. [PubMed: 21792049]
20. Euvrard S, Morelon E, Rostaing L, Goffin E, Brocard A, Tromme I, et al. Sirolimus and secondary skin-cancer prevention in kidney transplantation. N Engl J Med. 2012; 367:329–339. [PubMed: 22830463]
21. Guba M, von Breitenbuch P, Steinbauer M, Koehl G, Flegel S, Hornung M, et al. Rapamycin inhibits primary and metastatic tumor growth by antiangiogenesis: involvement of vascular endothelial growth factor. Nat Med. 2002; 8:128–135. [PubMed: 11821896]
22. Nathan N, Wang JA, Li S, Cowen EW, Haughey M, Moss J, et al. Improvement of tuberous sclerosis complex (TSC) skin tumors during long-term treatment with oral sirolimus. J Am Acad Dermatol. 2015; 73:802–808. [PubMed: 26365597]
23. Ormerod AD, Shah SA, Copeland P, Omar G, Winfield A. Treatment of psoriasis with topical sirolimus: preclinical development and a randomized, double-blind trial. Br J Dermatol. 2005; 152:758–764. [PubMed: 15840110]
24. Diaz-Ley B, Grillo E, Rios-Buceta L, Paoli J, Moreno C, Vano-Galvan S, et al. Classic Kaposi's sarcoma treated with topical rapamycin. Dermatol Ther. 2015; 28:40–43. [PubMed: 25314592]
25. Dickinson SE, Olson ER, Zhang J, Cooper SJ, Melton T, Criswell PJ, et al. p38 MAP kinase plays a functional role in UVB-induced mouse skin carcinogenesis. Mol Carcinog. 2011; 50:469–478. [PubMed: 21268131]
26. Baldelli E, Bellezza G, Haura EB, Crino L, Cress WD, Deng J, et al. Functional signaling pathway analysis of lung adenocarcinomas identifies novel therapeutic targets for KRAS mutant tumors. Oncotarget. 2015; 6:32368–32379. [PubMed: 26468985]
27. Rzeznicka II, Sovago M, Backus EH, Bonn M, Yamada T, Kobayashi T, et al. Duramycin-induced destabilization of a phosphatidylethanolamine monolayer at the air-water interface observed by vibrational sum-frequency generation spectroscopy. Langmuir. 2010; 26:16055–16062. [PubMed: 20873825]
28. Zebedin E, Koenig X, Radenkovic M, Pankevych H, Todt H, Freissmuth M, et al. Effects of duramycin on cardiac voltage-gated ion channels. Naunyn Schmiedebergs Arch Pharmacol. 2008; 377:87–100. [PubMed: 18176799]

29. Zhao M, Li Z. A single-step kit formulation for the (99m)Tc-labeling of HYNIC-Duramycin. Nucl Med Biol. 2012; 39:1006–1011. [PubMed: 22858374]
30. Zhao M, Li Z, Bugenhagen S. 99mTc-labeled duramycin as a novel phosphatidylethanolamine-binding molecular probe. J Nucl Med. 2008; 49:1345–1352. [PubMed: 18632826]
31. Boukamp P, Petrussevska RT, Breitkreutz D, Hornung J, Markham A, Fusenig NE. Normal keratinization in a spontaneously immortalized aneuploid human keratinocyte cell line. J Cell Biol. 1988; 106:761–771. [PubMed: 2450098]
32. Ehrhart JC, Gosselet FP, Culerrier RM, Sarasin A. UVB-induced mutations in human key gatekeeper genes governing signalling pathways and consequences for skin tumourigenesis. Photochem Photobiol Sci. 2003; 2:825–834. [PubMed: 14521217]
33. Lehman TA, Modali R, Boukamp P, Stanek J, Bennett WP, Welsh JA, et al. p53 mutations in human immortalized epithelial cell lines. Carcinogenesis. 1993; 14:833–839. [PubMed: 8504475]
34. Dickinson SE, Olson ER, Levenson C, Janda J, Rusche JJ, Alberts DS, et al. A novel chemopreventive mechanism for a traditional medicine: East Indian sandalwood oil induces autophagy and cell death in proliferating keratinocytes. Arch Biochem Biophys. 2014; 558:143–152. [PubMed: 25004464]
35. Sully K, Akinduro O, Philpott MP, Naeem AS, Harwood CA, Reeve VE, et al. The mTOR inhibitor rapamycin opposes carcinogenic changes to epidermal Akt1/PKBalpha isoform signaling. Oncogene. 2013; 32:3254–3262. [PubMed: 22890326]
36. Moses SA, Ali MA, Zuohe S, Du-Cuny L, Zhou LL, Lemos R, et al. In vitro and in vivo activity of novel small-molecule inhibitors targeting the pleckstrin homology domain of protein kinase B/AKT. Cancer Res. 2009; 69:5073–5081. [PubMed: 19491272]
37. Meuillet EJ, Zuohe S, Lemos R, Ihle N, Kingston J, Watkins R, et al. Molecular pharmacology and antitumor activity of PHT-427, a novel Akt/phosphatidylinositide-dependent protein kinase 1 pleckstrin homology domain inhibitor. Mol Cancer Ther. 2010; 9:706–717. [PubMed: 20197390]
38. Duncan FJ, Wulff BC, Tober KL, Ferketich AK, Martin J, Thomas-Ahner JM, et al. Clinically relevant immunosuppressants influence UVB-induced tumor size through effects on inflammation and angiogenesis. Am J Transplant. 2007; 7:2693–2703. [PubMed: 17941958]
39. Wulff BC, Kusewitt DF, VanBuskirk AM, Thomas-Ahner JM, Duncan FJ, Oberyszyn TM. Sirolimus reduces the incidence and progression of UVB-induced skin cancer in SKH mice even with co-administration of cyclosporine A. J Invest Dermatol. 2008; 128:2467–2473. [PubMed: 18463679]
40. de Gruijl FR, Koehl GE, Voskamp P, Strik A, Rebel HG, Gaumann A, et al. Early and late effects of the immunosuppressants rapamycin and mycophenolate mofetil on UV carcinogenesis. Int J Cancer. 2010; 127:796–804. [PubMed: 19998342]
41. Checkley LA, Rho O, Moore T, Hursting S, DiGiovanni J. Rapamycin is a potent inhibitor of skin tumor promotion by 12-O-tetradecanoylphorbol-13-acetate. Cancer Prev Res (Phila). 2011; 4:1011–1020. [PubMed: 21733825]
42. Zhang JF, Liu JJ, Lu MQ, Cai CJ, Yang Y, Li H, et al. Rapamycin inhibits cell growth by induction of apoptosis on hepatocellular carcinoma cells in vitro. Transpl Immunol. 2007; 17:162–168. [PubMed: 17331842]
43. Wang YD, Su YJ, Li JY, Yao XC, Liang GJ. Rapamycin, an mTOR inhibitor, induced apoptosis via independent mitochondrial and death receptor pathway in retinoblastoma Y79 cell. Int J Clin Exp Med. 2015; 8:10723–10730. [PubMed: 26379864]
44. Rozengurt E, Soares HP, Sinnet-Smith J. Suppression of feedback loops mediated by PI3K/mTOR induces multiple overactivation of compensatory pathways: an unintended consequence leading to drug resistance. Mol Cancer Ther. 2014; 13:2477–2488. [PubMed: 25323681]
45. O'Reilly KE, Rojo F, She QB, Solit D, Mills GB, Smith D, et al. mTOR inhibition induces upstream receptor tyrosine kinase signaling and activates Akt. Cancer Res. 2006; 66:1500–1508. [PubMed: 16452206]
46. Voskamp P, Bodmann CA, Koehl GE, Tensen CP, Bavinck JN, Willemze R, et al. No acceleration of UV-induced skin carcinogenesis from evenly spread dietary intake of cyclosporine in contrast to oral bolus dosages. Transplantation. 2013; 96:871–876. [PubMed: 23958926]

47. Cernysiov V, Gerasimcik N, Mauricas M, Girkontaite I. Regulation of T-cell-independent and T-cell-dependent antibody production by circadian rhythm and melatonin. Int Immunol. 2010; 22:25–34. [PubMed: 19946015]

48. Fortier EE, Rooney J, Dardente H, Hardy MP, Labrecque N, Cermakian N. Circadian variation of the response of T cells to antigen. J Immunol. 2011; 187:6291–6300. [PubMed: 22075697]

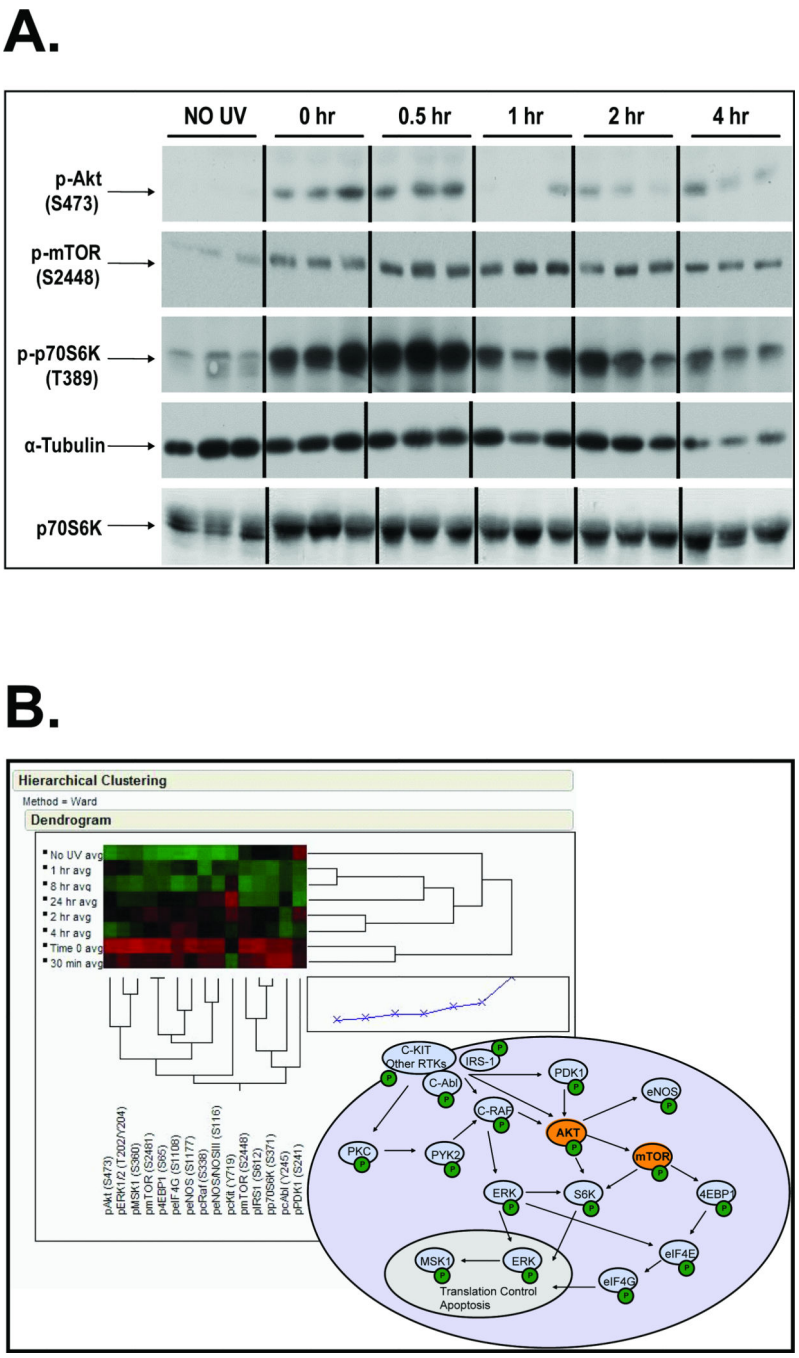

Figure 1. Solar simulated light(SSL) induces mTOR/Akt-related signaling events in mouse epidermis

SKH-1 hairless mice (n=3) were acutely irradiated with 105 kJ/m^2 UVA/6.4 kJ/m^2 UVB and sacrificed at the indicated times (0 hr refers to mice that were irradiated and immediately sacrificed). Epidermal proteins were analyzed by Western blotting (A) or reverse phase protein microarray (RPPA, B). The heat map represents the average of the three independently analyzed samples per timepoint (0hr, 30 min, 1hr, 2hr, 4hr, 8hr and 24hr). The signaling diagram represents some of the proposed signaling pathways activated by solar-simulated light based on data obtained through the RPPA analysis.

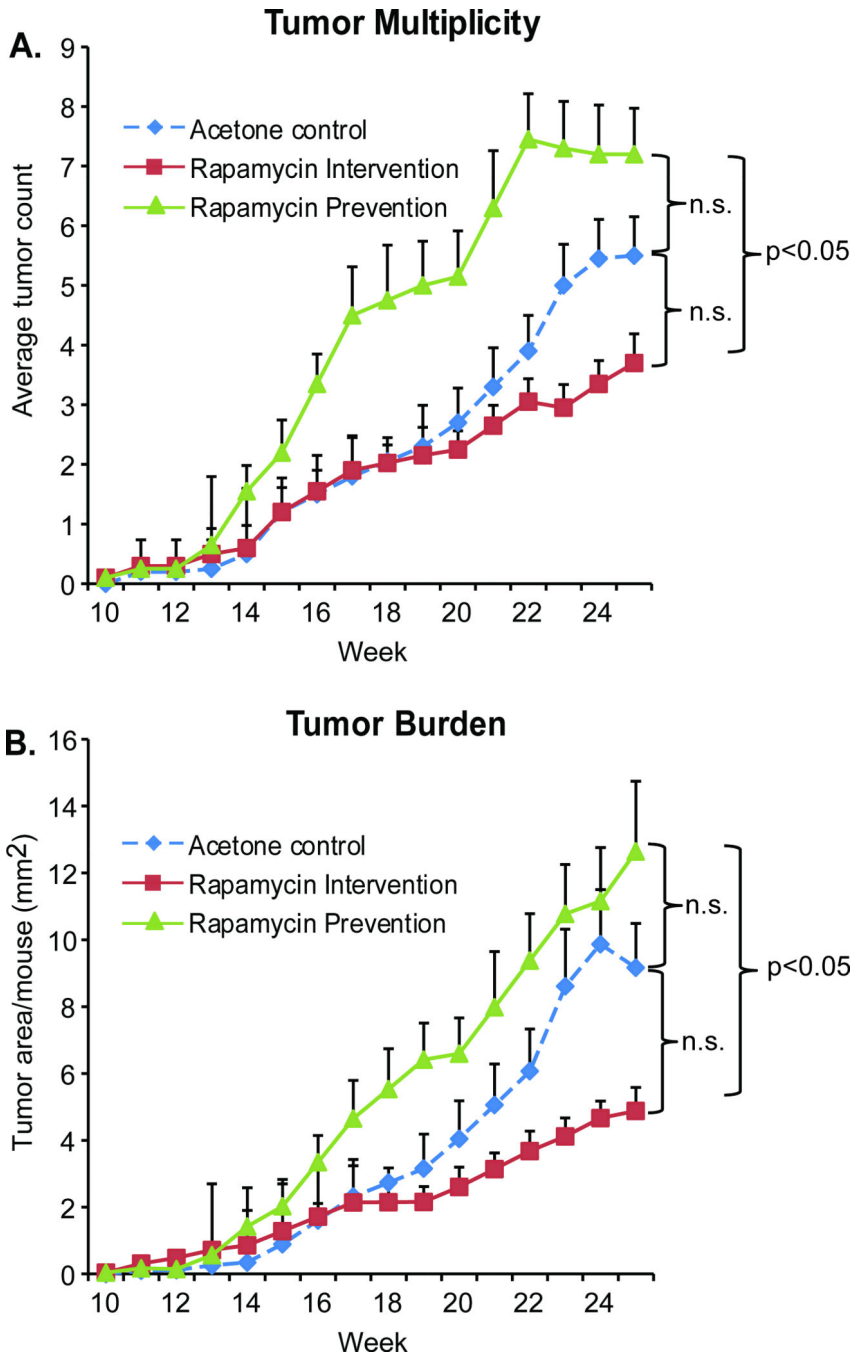

Figure 2. Treatment schedule of topical rapamycin application affects the outcome of solar simulated light-induced skin tumorigenesis

SKH-1 hairless female mice were treated with solar simulated light (SSL) 3 times a week for 15 weeks (n = 20). Control mice were treated on their back skin with vehicle (acetone) 1hr prior to each UV exposure, and continued with 3× weekly acetone treatments after UV stopped. Mice in the “Prevention” group were treated 3 times a week with rapamycin (50nmol/back) 1 hr prior to UV exposure, and continued receiving this treatment after SSL stopped. Mice in the “Intervention” group received only vehicle (acetone) 1hr prior to each SSL treatment, but switched to treatments with rapamycin after SSL stopped. All mice were

observed for tumor number and size until sacrifice at week 25, at which point tissues were harvested. Tumor multiplicity (average number of tumors per mouse) is shown in A. Tumor burden (average area per mouse) is shown in B. Data are shown as mean values + SEM.

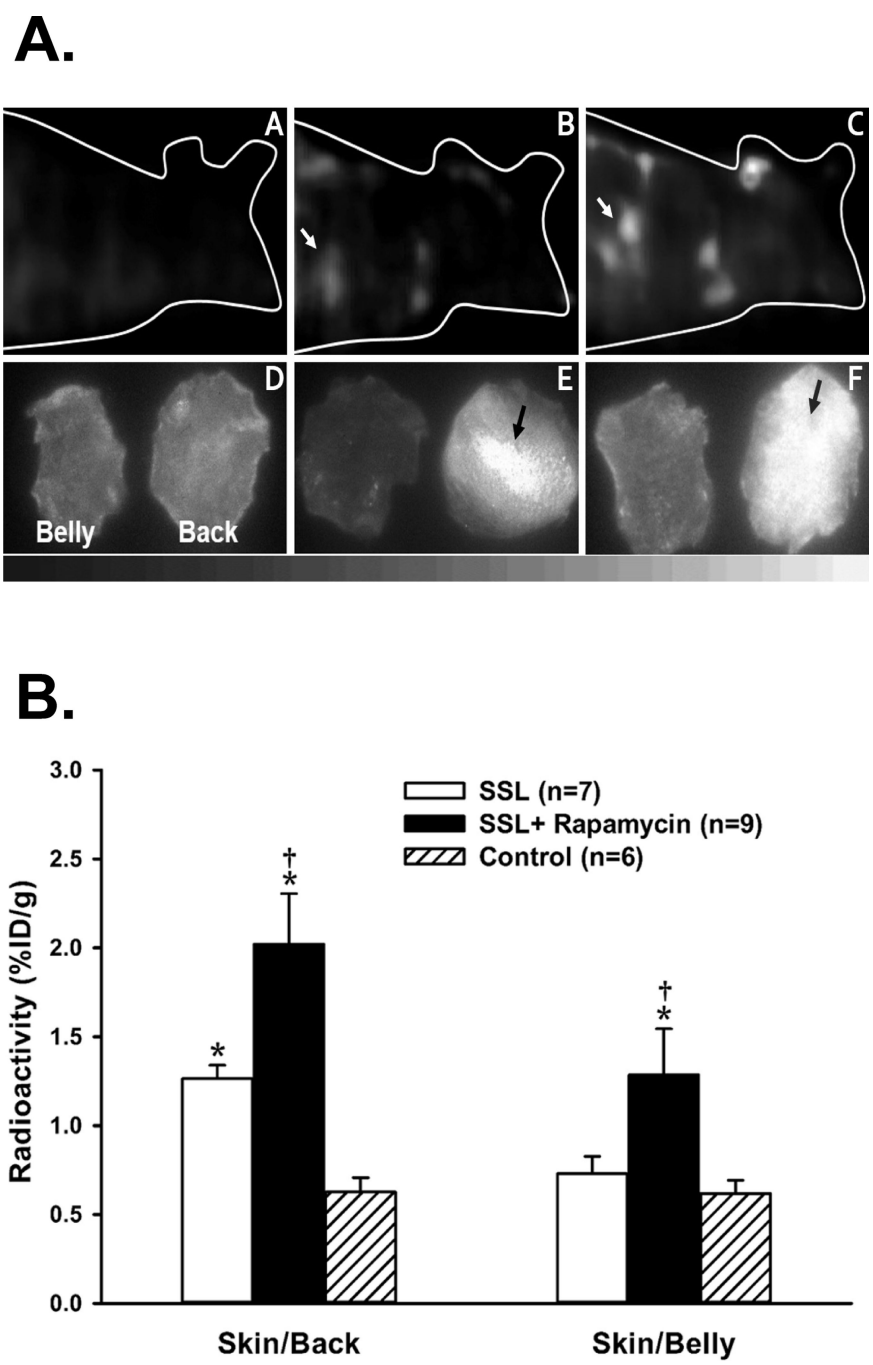

Figure 3. Topical treatment with rapamycin potentiates acute SSL-induced apoptotic signaling *in vivo*

3A. *Top row*: Volume rendering displays of ^{99m}Tc-duramycin SPECT images in SKH-1 mice representative of untreated control (A), vehicle control with SSL (B), and rapamycin treatment with SSL (C). Mice were imaged 48 hours after SSL exposure. *Bottom row:* Autoradiograph images of the back skin (right) and belly skin (left) collected from animals presented above in the top row. The images labeled by D, E, and F are collected from corresponding A, B, and C mice, respectively. Multiple lesions (arrows) of increased

radioactive uptake (hot spots) were predominantly visualized on the back skin of the mice receiving SSL exposure with rapamycin treatment (F), less in that of mice receiving SSL with vehicle treatment (E), and not on the skin of control mice. **3B.** Results of ^{99m}Tc-duramycin *ex vivo* biodistribution measurements of control, SSL with vehicle, and SSL with rapamycin treatment groups at 2 hours after radiotracer injection. * = $P < 0.01$ compared to Control; † = $P < 0.01$ compared to SSL.

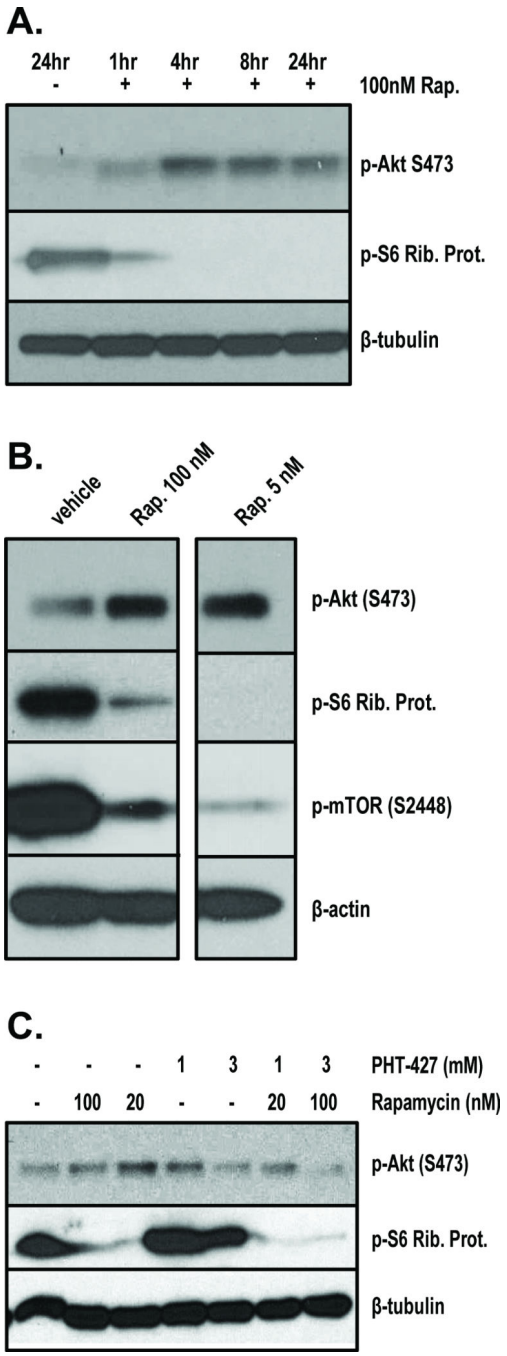

Figure 4. Rapamycin treatment causes increased Akt signaling in cultured keratinocytes which is blocked by PHT-427

Primary human keratinocytes were exposed to either 100nM rapamycin over a timecourse (A), or differing doses of Rapamycin for 24hr (B) and then harvested for Western blot analysis, 20ug per lane. Blots were probed for p-Akt (S473), p-S6 Ribosomal Protein, or beta tubulin as a loading control. HaCaT human keratinocytes were grown to 70% confluence and then treated with rapamycin, PHT-427, or both in serum-free media at the indicated doses. After 24hr the cells were lysed and processed for Western blot analysis,

20ug per lane (C). Blots were probed for p-Akt (S473), p-S6 Ribosomal Protein or beta tubulin as a loading control.

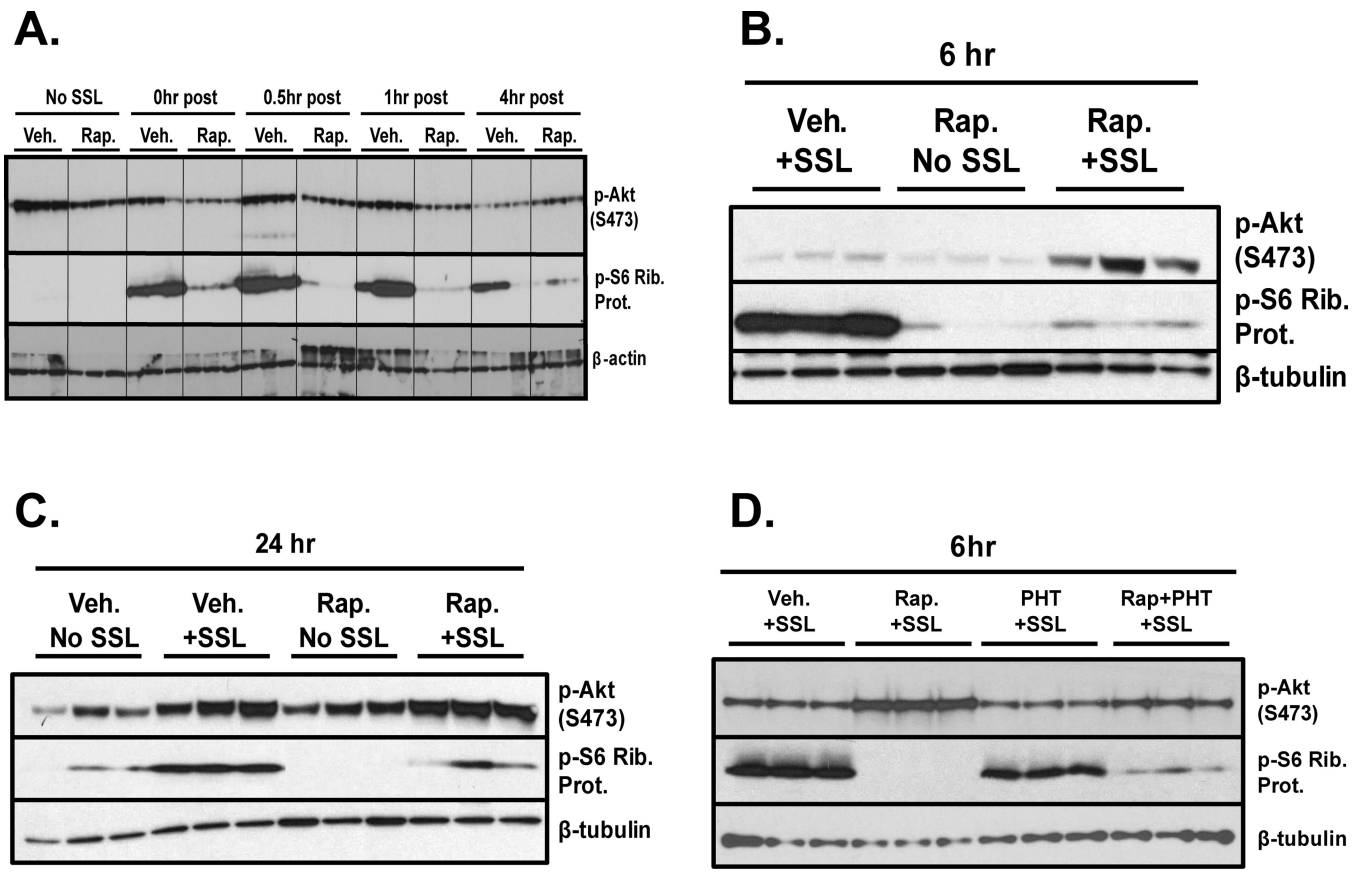

Figure 5. Topical treatment with rapamycin prior to SSL causes hyperphosphorylation of Akt (S473) in mouse epidermis which is inhibited by PHT-427

Female SKH-1 hairless mice (n = 3) were pretreated three times (48hr, 24hr, and 1hr) with rapamycin (50nmol/back) prior to acute solar simulated light (SSL) treatment at the dose used in Figure 1. Mice were then sacrificed along a timecourse up to 4hr and epidermal proteins were extracted for Western blot analysis (0hr indicates sacrifice immediately after UV exposure, A). To confirm the delayed hyperphosphorylation of Akt (S473) after SSL in the presence of rapamycin, new mice were treated as described above and harvested at 6hr and 24hr post SSL for Western blot analysis of epidermal lysates (B, C). A third acute mouse experiment was performed to test the effects of PHT-427 on p-Akt (S473) in SSL-exposed epidermis. Mice were treated with rapamycin or PHT-427 (3.7umol/back) or both as described above and harvested 6hr post SSL exposure. Epidermal lysates were blotted for p-Akt (S473), p-S6 Ribosomal Protein or beta-tubulin as a loading control.

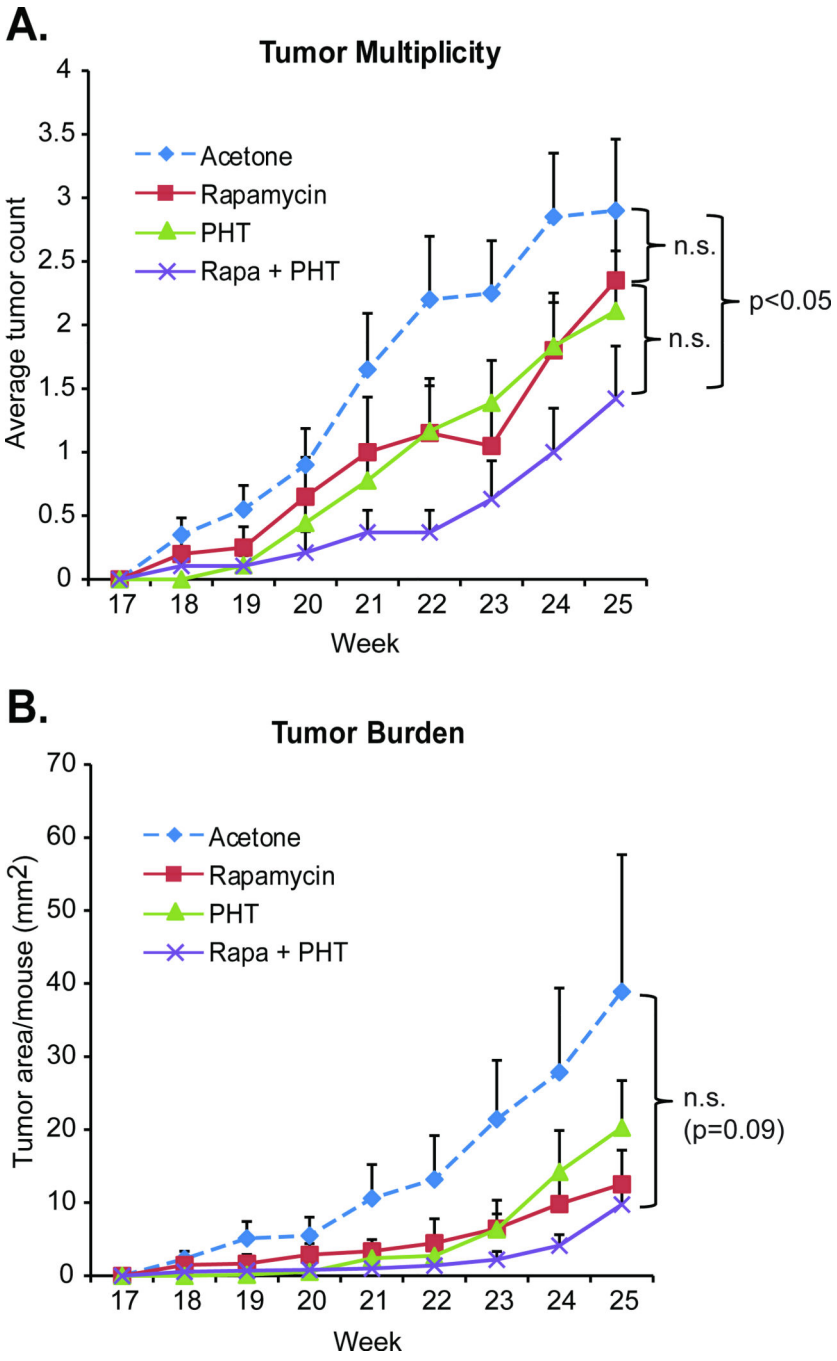

Figure 6. PHT-427 additively contributes to skin tumor inhibition when combined with rapamycin

SKH-1 hairless female mice were treated 3 times a week for 15 weeks with SSL. After 15 weeks UV treatments stopped and mice were split into four groups (n = 20). Mice were then treated topically on their backs three times a week for an additional 10 weeks with either vehicle (acetone), rapamycin (50 nmol/back), PHT-427 (3.7umol/back) or both agents (same doses). All mice were observed for tumor number and size until sacrifice at week 25. Tumor

multiplicity (average number of tumors per mouse) is shown in A. Tumor burden (average area per mouse) is shown in B. Data are shown as mean values + SEM.